SKOG FORSK Arbetsrapport

Nr 364
1997

Dynamics of Forestry Machines

Björn Löfgren

SkogForsk, Glunten, 751 83 UPPSALA • Tel: 018-18 85 00 • Fax: 018-18 86 00
skogforsk@skogforsk.se • http://www.skogforsk.se

Front picture: Simulation model of Valmet 840
Illustrator: Björn Löfgren

SkogForsk - The Forestry Research Institute of Sweden
pursues research and development aimed at long-term, economical, ecologically sound forestry. SkogForsk is supported by the entire forestry sector in Sweden through member fees and a charge levied on each cubic meter of wood harvested. Financial support is also given by the government according to a special agreement and by scientific funds for certain projects. Research and development is carried out in four main areas: Raw materials and the wood market, Silviculture and conservation, Breeding and propagation, and Operations systems. In addition to this, SkogForsk performs contract research for forest enterprises, machine manufacturers, and authorities.

Our series Work Reports are documenting long term trials, inventories, studies, etc. and are only distributed on order.

Results from the research and development work are regularly published in the following series:

SkogForsk-Nytt and the English edition *SkogForsk-News:* News, summaries, surveys.
Resultat and *Results:* Conclusions and recommendations in a light accessible form.
Redogörelse: Comprehensive reports in Swedish on completed R&D projects.
Reports: Reports in English on research work and methods.

Handledningar and *Manuals:* Practical advice and guidelines for different operations. A few in English.

Contents

Summary

The forest machines of today are derived from the basic farm tractor pulling a semitrailer. Forest machines have been developed mainly to achieve high terrain accessibility, a good carrying capacity and a high traction force. As a result, most such machines are large and heavy, with big engines and transmissions.

These developments have led to the production of machines with good accessibility and carrying capacity. On the other hand, forest machines have become very heavy and tend to be designed for dealing with extreme terrain types.

No one has yet to do any research on how the dynamics of forest machines affects their construction or ground pressure. The dynamics of a forest machine involves a complex of interactions between the tyres and ground which are influenced by terrain variation and changes in machine design. Some of the parameters could, for example, be

- the weight of the machine
- the dimensions and geometry of the machine
- the dynamics of the machine
- the driveline of the machine
- the design and behaviour of tyres

The main objective of this study was to better understand the interaction between the forest machine and the ground when driving over the terrain. Another objective was to create a modelling tool which could be used as a basis for further work aimed at developing more lenient forest machines.

A new simulation model for describing the dynamic behaviour of a forwarder has been introduced. The model consists of three major parts:

- the machine model
- the tyre model

A 3D tyre model for off-road application has been introduced. The model is capable of simulating runs over uneven obstacles such as stones. The model can predict vertical, lateral and longitudinal forces of the tyre. In its present form it should be suitable for running some common types of forest machine simulations. One of its main attractions is the small amount of simply obtained experimental data that it demands. Based on comparisons with tyre test data it can be concluded that the tyre model duplicates the enveloping characteristics of the forest tyre. However, verification has only been achieved for low-speed tyre excursions. The importance of high-rolling-speed tyres in terms of the contribution of carcass dynamics to net tyre loads is not known.

Background

The forest machines of today are derived from the basic farm tractor-semi-trailer combination. Forest machines have been developed mainly to achieve high terrain accessibility, a good carrying capacity and a high traction force. Consequently, most such machines are large and heavy, with big engines and transmissions.

To obtain an even higher tractive effort, large, hard inflated tyres with aggressive threads are commonly used, and if this not enough, one can also use an anti-skid device. To increase terrain accessibility, articulated steering and bogies were developed, first on the rear part of the machines and later on the front.

These developments have resulted in machines with good accessibility and a high carrying capacity. On the other hand, forest machines have become very heavy, and most are designed for use under extreme terrain situations.

The widespread adoption of mechanised thinning and cleaning during the 1980s has placed new demands on forest machines. Thus modern machines will require good terrain accessibility and good manoeuvrability which results in less damage and greater flexibility in the choice driving routes in the forest. Driving in connection with thinning work can easily cause damage to the ground, such as soil compaction and rut formation, as well as damage to roots and stems of the residual stand. Often the degree of damage varies depending on the construction of the forest machines (Olsen, 1989).

Lot of tests (Hallonborg, 1983; Löfgren, 1991; Myhrman & Karlsson, 1990) have been carried out to measure rut depths and evaluate accessibility on soft ground. These types of tests are limited to comparing existing forest machines and ranking them in terms of their impact.

All empirical tests have two main types of weaknesses: Only existing configurations can be evaluated, and tests only be carried out once in a given area since the ground is disturbed by the test. Thus one cannot run a series of comparative tests in the same area.

It has only been during the last few years that researchers in Sweden have been studying how slip affects ground impact (Friman et al. 1991). No one has up to now done any research on how the dynamics of the forest machines affects machine construction and ground pressure. The dynamics of a forest machine involves a complex of interactions between the tyres and ground which are influenced by terrain variation and changes in machine design. Some of the parameters could, for example, be

- the weight of the machine
- the dimensions and geometry of the machine
- the dynamics of the machine
- the driveline of the machine
- the design and behaviour of tyres

The forest machine can be modelled as a number of rigid bodies connected to each other by joints. The only parts of the machines that have any dynamic characteristics are the tyres. Fig. 1 shows the connection between the machine and ground.

Figure 1.
Description of the interaction between machine and ground.

A proper tyre model, describing the tyre forces, is essential for modelling the dynamic behaviour of a forest machine in uneven terrain.

Objectives

The main objective of this study was to better understand the interaction between the forest machine and the ground when driving over the terrain.

More specifically, the objective was to develop the knowledge base needed to create a tyre model that can be applied to uneven terrain with obstacles. At this stage a tyre model will be developed for hard ground only.

Another objective was to create an modelling tool which could be used as a basis for further work aimed at developing more lenient forest machines.

Literature

The complexity of the structure and behaviour of tyres has forced many researchers to idealise tyre characteristics and develop a number of simplified mathematical models that each have a specific purpose and limited applicability. Relationships between the longitudinal, lateral, and normal forces as well as tyre forces were developed in these models.

The survey begins with an description of existing tyre models in the ADAMS simulation software and their limitations.

Tyre models in ADAMS

There are four different tyre models available in the ADAMS software package (Anon., 1994*)*. The models are divided into two groups:

- analytical models
- experimental models.

Analytical models

Three of the tyre models are analytical, representing tire – terrain interactions as a set of forces that may be written as analytical functions of the deformation parameters. The three tyre models are:

- The simple-equation-and-equivalent-plane tyre model
- The Fiala tyre model
- The University of Arizona tyre model.

The tyre co-ordinate system employed by ADAMS/tyre is identical to that defined by the Society of Automotive Engineers (SAE), see Fig. 2.

Figure 2.
SAE Tyre co-ordinate system

The simple-equation-and-equivalent-plane tyre model

The equivalent plane method is based on a radial spring tyre model (Davis, 1974) Fig. 3.

Figure 3.
Radial-spring tyre model.

Assumptions made in the tyre model:

- The tyre is a thin, circular disk that deforms only in a radial direction.
- The terrain is deformable.
- The tyre radial force deformation relationship on a rigid planar surface is known.

The tyre model redefines the terrain as an equivalent ground plane which reflects both the elevation and the slope characteristics of the original terrain contacting the tyre, Fig. 4.

Figure 4.
Segmented tyre on rigid surface

For a tyre on a rigid planar surface, the tyre area displaced by the terrain and the arc of the contact patch together with the tyre force-deformation curve determine the magnitude of the radial tyre force.

Limitations

The equivalent plane method is best suited for relatively large obstacles because it assumes that the tire encompasses the obstacles uniformly. In reality, the pneumatics and the bending stiffness of the tire carcass prevent this. The result is an uneven pressure distribution, and gaps may occur between the tire and the road. If the obstacle is larger than the tire contact patch, the uniform assumption is valid. If the obstacle is much smaller than the tire patch, however, the assumption is invalid, and the equivalent plane method may greatly underestimate the durability force. The durability tire force model is also limited to two-dimensional forces that lie in the wheel-centre plane.

Fiala tyre model

Fiala (1964) introduced a spring-bedded ring model to represent the tyre structure, shown in Fig 5. The tread band structure of the tyre is assumed to have characteristics of a beam attached to the elastic structure of the side walls. Between the tread band and the road surface, the rubber is assumed to act as a series of separate radial strips of rubber.

Figure 5.
Fiala tyre model.

The following assumptions are made in ADAMS:

- rectangular contact patch or footprint
- pressure distribution uniform across contact patch.
- tyre modelled as a beam on a elastic foundation

Limitations

The Fiala tyre model is used for simple manoeuvres where the inclination angle is not a major factor and where longitudinal and lateral slip effects can be considered unrelated. The Fiala model is only two-dimensional and is used for handling analyses. It is unsuitable for use on uneven terrain.

The University of Arizona model

The following assumptions are made in ADAMS:

- rectangular contact path or footprint
- pressure distribution parabolic across contact path
- tyre modelled as beam on an elastic foundation.

Experimental models

- Two of the tyre models in ADAMS are experimental:
- the interpolation and point follower
- the Smithers tyre model.

The Smithers tyre model is based partly on experimental data and partly on analysis. The model is called “Smithers” because Smithers Scientific Services Inc. provides the experimental data and the fitting techniques for computing the lateral force and aligning torque.

The Smithers technique uses the “Magic Formula“ for computing lateral force and aligning torque. The Fiala analytical method is used for computing all other forces and torque’s.

Limitations

You need a lot of tyre data from tests made by Smithers, and you cannot use the load-deflection data from the tyre manufacture. The extended Smithers model is only two-dimensional and is used for handling analyses and comprehensive slip. It is not suitable for use on uneven terrain.

Terrain model in ADAMS

The terrain model (ANON., 1994) is a general three-dimensional surface that is defined as a series of triangular patches as shown in Fig. 6.

Figure 6.
Terrain representation in ADAMS.

Figure 6 depicts a road surface formed by six nodes, numbered 1 through 6. The six nodes together form a triangular patch element denoted as A, B, C, and D. The unit outward normal for each triangular patch is shown for the

sake of clarity. The road is specified by the co-ordinates of each node in a specified co-ordinate system. Subsequently, the connectivity defining each triangular patch is specified. For each triangular patch, separate friction properties may also be specified.

Limitations

The tyre-road contact algorithm detects no more than two simultaneous element contact If the tyre contacts three or more surfaces simultaneously, the tyre-road contact algorithm only detects and accounts for two, and these two will not necessarily be the most important two.

Tyre models for off-road

In a survey (Löfgren, 1992) different tyre models are discussed for use in off-road applications. The survey discusses three types of tyre models

- empirical models
- semi-empirical models
- analytical models

A model proposed by Baladi (1984) is recommended for use in modelling the soil-tyre interaction in simulations involving forestry machines. The model describes the interaction between the tyre as two springs in series, one describing the flexibility of the tyre and the other describing the strength of the soil, figure 7.

Figure 7.
Soil-tyre model proposed by Baladi.

Tyre models on hard ground

Tyre models can be classified into three distinct categories:

- empirical
- analytical
- finite element models

More emphasis is put on the discussion of analytical models. These types of models are more suitable for use in off-road applications and uneven terrain. Dynamic data are almost impossible to get from tyres in uneven terrain. Empirical models have been developed on the basis of dynamic data on rolling tyres, while analytical models are based mainly on data obtained in the static modelling of tyre structure. Even though empirical models, such as ”The Magic Formula (Pacejka, 1993) give a more realistic response in simulations, empirical models are used more for vehicle handling analyses on flat roads.

In the survey (Löfgren, 1992) four different models based on the point-contact-model are presented. These types of models are limited in the way that they give poor estimates of a rough terrain, small wavelength bumps are filtered out, and the contact area is unaffected by the tyre deflection. The forces in these models are predicted based on the assumption that the resultant tyre force is always normal to the local ground profile.

Another commonly used idea is to use angular distributed, independent, linear radial spring elements (Davis, 1974, Baladi, 1984, Ingham, 1973), Fig. 8.

Figure 8.
Tyre model with radial spring elements.

The forces in radial-spring tyre models result from the summation of the vertical and horizontal components of force in each element due to local radial spring deflection.

Radial-spring tyre models can be used to calculate the tire envelopment of small surface obstacles. Each radial spring element is independent of its neighbour’s deflection.

A tyre model that accounts for the radial element deflection dependence upon their neighbours deflection is presented of Baladi et al. (1984). The model is based on radial-interradial springs, figure 9.

Figure 9.
Radial-interradial spring tyre model.

Two tyre models are analysed: the linear radial-linear interradial model and quadratic radial-linear interradial model. The tyre model based on quadratic radial-linear interradial idea performs best in tests where the tyre is run over an obstacle.

Methodology

This chapter describes a new tyre model for off-road analyses and a new way to represent the terrain in ADAMS. The ADAMS model of a forwarder is also described.

Tyre model

The ultimate aim of the tyre model is not to describe or study the actual tyre dynamics, but rather to incorporate the tyre model into the simulation of a forestry machine dynamics, thereby providing a better prediction technique for studying the total forestry machine. A simple tyre simulation model should be based on force-deflection data from tyre manufactures. Ground-stiffness data should be based on cone penetrometer values. In forestry machine simulations the tyre model could be based on static data since the speed of forestry machines is very low, 0.2 – 1.5 m/s.

In existing tyre models, the tyre is treated as a thin disc in two dimensions associated with a contact patch described as a toriod membrane (Hallonborg,

1996) or a rectangular patch (Anon., ***??***). This will cause a problem in off-road applications, especially in those related to forestry. The tyres mounted on forestry machines are wide (600–800 mm). This means that there will often be partial contact between the tyres and obstacles that have no uniform propagation**,** see figure 10.

Figure 10.
Partial contact between a tyre and an obstacle

The literature survey shows that a tyre model based on radial spring would suit off-road simulations in the sense of treating obstacles and ground deformation. The proposed tyre model is based on the quadratic radial-linear interradial model by Badalamenti (1988). The new tyre model is extended from 2D to 3D and also includes lateral forces, longitudinal forces, slip and shear forces. In this thesis the tyre model only deals with tyres on hard, uneven ground.

Tyre forces and moment

To describe the behaviour of tyres and the forces acting on them, it is necessary to define an axis system that serves as a reference for defining various parameters. The co-ordinate system used is based on a proposed standard by ISO, Fig. 11.

Figure 11.
Axes, forces and torque's.

The tyre model calculates three orthogonal forces and the three orthogonal torque's (figure 11) that result from conditions at the tire-road surface contact patch. All forces and torque's are applied at the centre of the wheel.

Figure 12.
Directional vectors for the application of tire forces and torque's at the tire-road surface contact patch.

Figure 13.
Tire forces and torque's applied at the wheel centre.

2D to 3D

To take the width of a forestry tyre and partial ground contact into account, the tyre model has been extended from one 2D-disc into a 3D-model consisting of five 2D-discs, see Fig. 14.

Figure 14.
The tyre divided into 5 discs.

The vertical force acting on each disc is given by:

$$F_{di} = F_{vtot} / 5 \qquad i = 1...5 \tag{1}$$

Figure 15.
The vertical force distribution on a 5-disc tyre.

One disc

For each 2D-disc the quadratic radial-linear interradial tyre model is used. The tyre quadratic radial-linear interradial model consists of quadratic radial springs and linear interradial springs. Fig. 16.

Figure 16.
Radial-interradial spring tyre model.

Figure 17.
Radial spring tyre element

The radial force in element *i*, Fig. 17, can be written as:

$$F_{ri} = k_1 d_{ri} + k_2 d_{ri}^2 + k(2d_{ri} - d_{ri-1} - d_{ri+1}) \quad i = 2,3,\ldots N-1 \tag{2}$$

$$F_{r1} = k_1 d_{r1} + k_2 d_{r1}^2 + k(d_{r1} - d_{r2}) \tag{3}$$

$$F_{rN} = k_1 d_{rN} + k_2 d_{rN}^2 + k(d_{rN} - d_{rN-1}) \tag{4}$$

The vertical force in element *i* is given by:

$$F_{vi} = F_{ri} \sin\theta_i \tag{5}$$

The total vertical force from one disc on the wheel axle due to *N* radial displacement is:

$$F_v = \sum_{i=2}^{N-1} [k_1 d_{vi} + k_2 d_{vi}^2 / \sin\theta_i + k(2d_{ri} - d_{ri-1} \sin\theta_i / \sin\theta_{i-1} - d_{ri+1} \sin\theta_i / \sin\theta_{i+1})]$$
$$+ k_1 (d_{v1} - d_{vN}) + k_2 (d_{vi}^2 / \sin\theta_i + d_{vN}^2 / \sin\theta_N) \tag{6}$$
$$+ k(d_{v1} + d_{vN} - d_{v2} \sin\theta_1 / \sin\theta_2 - d_{vN-1} \sin\theta_N / \sin\theta_{N-1})$$

where d_i is given by:

d_{vi} h_i r $_i$ h_{gi}

$=$ $-$ $(1 - \sin\theta\ ) -$ (7)

The spring constants have to be determined by the tyre force-deflection curves.

The total vertical force on the wheel axle due to 5 discs is:

$$F_{vtot} = \sum_{i=1}^{5} F_{vi} \tag{8}$$

where F_{vi} is given by equation (6).

There are three main forces acting on the tyre from the ground: the longitudinal force, f_x, which is the component in the x direction of resultant force acting on the tyre; the lateral force, f_y, which is the component in the y direction of resultant force acting on the tyre; and the normal force, f_z, which is the component in the z direction of resultant force acting on the tyre from the load.

Longitudinal force

Longitudinal tyre force results from traction or braking and depends primarily on the longitudinal slip of rotating tyres. Longitudinal slip is the ratio of the difference between the tyre translational speed and the free rolling speed to the translational speed *v*. The slip is given by:

$$s_t = \frac{r_r\omega - v}{r_r\omega} \quad \text{traction} \tag{9}$$

$$0 < s < 1 \tag{10}$$

$$s_b = \frac{v - r_r\omega}{v} \quad \text{braking}$$

$$-1 < s < 0$$

The circumferential speed ωr_r of the spring element i in each disc is given by:

$$wri = (r_i - d_{ri})\omega \qquad i = 1....n \tag{11}$$

where:

$$d_{ri} > 0$$

As a result the slip will differ along the circumference of each disc. Therefore the mean value of the circumferential speed will be calculated. For each disc this value is given by:

$$\omega r_r = \frac{\omega \sum_{i=1}^{N} \sin(\theta_i)(r_i - \delta_{ri})}{m} \tag{12}$$

where: m = number of elements where $\delta_i > 0$

The slip ratio influences the longitudinal force F_x through its effect on the circumferential coefficient of friction. The force F_x is taken also to be proportional to the normal load F_z and therefore given by:

$$F_x = \mu(s)F_z \tag{13}$$

where $\mu(s)$ is approximated by a functional relationship representing the friction coefficient slip behaviour. The coefficient of friction is given by the following equation:

$$\mu(s) = \mu_0(1 - as - e^{-bs}) \tag{14}$$

a and b are constansts.

Figure 18.
Longitudinal coefficient of friction.

Figure 19.
Spring element in contact with an obstacle in x-z plane.

The longitudinal force F_x for each spring element is given by:

$$F_{xi} = F_{gi} \cos \phi_i \tag{15}$$

$$F_{gi} = \mu(s)_i F_{ri} \cos(\gamma_i) \tag{16}$$

$$F_{xi} = \mu(s)_i F_{ri} \cos(\gamma_i) \cos\phi_i \tag{17}$$

$$\phi_i = \arctan\left(\frac{dz}{dx}\right) \tag{18}$$

The total longitudinal force on the wheel axle from one disc due to N radial displacement is:

$$F_x = \sum_{i=1}^{N} \mu(s)_i F_{ri} \cos(\gamma_i) \cos\phi_i \tag{19}$$

The total longitudinal force on the wheel axle due to 5 discs is:

$$F_{xtot} = \sum_{i=1}^{5} F_{xi} \tag{20}$$

Lateral force

In uneven terrain, such as in off-road applications, there are, in principal, two cases where lateral forces can occur, i.e. when driving on an inclined surface, which generates lateral forces, and when steering. There are also combinations of these cases, i.e. inclined surface and steering,

Inclined surface

On ground with an inclined, hard surface and no steering the lateral force is given by:

$$F_y = \mu F_z \tag{21}$$

The slip ratio influences the lateral force F_y through its effect on the circumferential coefficient of friction. In addition, the force F_y is taken to be proportional to the normal load F_z and therefore given by:

$$F_y = \mu(s) F_z \tag{22}$$

Figure 20.
Spring element in contact with an obstacle in y-z plane.

The lateral force F_y for each spring element is given by:

$$F_{yi} = F_{gi} \cos \xi_i \tag{23}$$

$$F_{gi} = \mu(s)_i F_{ri} \cos(\chi_i) \tag{24}$$

$$F_{yi} = \mu(s)_i F_{ri} \cos(\chi_i) \cos \xi_i \tag{25}$$

$$\xi_i = \arctan\left(\frac{dz}{dy}\right) \tag{26}$$

The total longitudinal force on the wheel axle from one disc due to N radial displacement is:

$$F_y = \sum_{i=1}^{N} \mu(s)_i F_{ri} \cos(\chi_i) \cos \xi_i \tag{27}$$

The total lateral force on the wheel axle due to 5 discs is:

$$F_{ytot} = \sum_{i=1}^{5} F_{yi} \tag{28}$$

Steering

When a rolling tyre is steered at an angle δ from the direction of wheel travel (x-direction), a lateral force will arise, and the vehicle will move laterally, Fig.21.

Figure 21.
Lateral force generation on the tyre.

Several analytical models have been developed using various approaches to formulate and solve the differential equations governing deformation of the tyre material. When a tyre rolls straight forward, as in Fig. 22a, the contact area is symmetrical relative to the wheel hub. At small steering angles, as in Fig. 22b, the contact area will move proportional to the steering angle and only a small part of the contact area will be a gliding zone. When the steering angle increases, as in Fig. 22c, the gliding zone increases, the lateral force moves to the axle centre, and the aligning torque decreases.

a **b** **c**

Figure 22.
Model of lateral force generation in a tyre.

The deformation in these regions produces stresses whose integration over the contact area represents the lateral force, located at a distance *t* (pneumatic trail) from the centre of the contact area. This offset in F_y produces the self-aligning torque. Many of the analytical models have never been used in simulations owing to a lack of data. Empirical models are primarily based on the statistical analysis of data collected from tyre testing. There is a need for more laboratory tests to get all the required tyre data. In our case it was not possible to obtained these data, so a simplified equation has been used to generate the lateral force:

$$F_y = \mu F_z (1 - e^{-K|\alpha|}) \tag{29}$$

Figure 23.
Tire lateral force equation.

Combined lateral and longitudinal forces

Under practical conditions, tyres are subjected to simultaneous cornering and braking effects. Under such conditions the tyre force model has to be modified to include this effect. The friction cake concept, introduced by Weber (1985), has been adopted in this tyre model. This concept is based on the assumption that tyre forces act in the same way as corresponding slip components:

$$F_y / \alpha = F_x / s = R / k \tag{30}$$

where R is the resultant force (vectorial sum of F_x and F_y) in the contact surface, and *k* is the vectorial sum addition α of and *s*.

$$R^2 = F_y^2 + F_x^2 \tag{31}$$

$$k^2 = \alpha^2 + s^2 \tag{32}$$

It is also assumed that the curve R(k) can be rotated to form a surface of revolution over the basic circle with radius k = 1. The procedure of determining tyre forces is that for a given longitudinal and lateral slip (s and α), and the basic curve of R versus k, the instantaneous resultant force is

R(k)

$$k = (\alpha^2 + s^2)^{1/2} \tag{33}$$

The force R is resolved into components F_x and F_y :

$$F_x = R\sin(\beta) \tag{34}$$

$$F_y = R\cos(\beta) \tag{35}$$

where

$$\beta = \arctan(\alpha / s) \tag{36}$$

Contact area

In the proposed tyre model two concepts of determining the contact area are used. One concept is used on ground with a flat, hard surface and the other on hard, uneven surfaces.

Flat ground

The contact area on ground with a flat, hard surface can be described as a super ellipse, Fig. 24.

Figure 24.
The contact area described as a super ellipse.

The equation of the super ellipse in an orthogonal co-ordinate system is:

$$\frac{x^n}{a^n} + \frac{y^n}{b^n} = 1 \tag{37}$$

where the exponent n is a positive real number which determines the shape of the curve. The parameters a and b determine the length and width, respectively, of the contact area, Fig. 25.

Figure 25.
Shape of the curve when $a = b = 1$ **and** $n = 1, 2, 2{,}5$ *and* 4.

On a flat, rigid surface the contact area can divided into four equal quadrants, Fig. 26.

Figure 26.
The contact area *divide into one quadrant.*

For the first quadrant the function $f(x)$ is given by

$$f(x) = b \cdot \left(1 - \frac{x^n}{a^n}\right)^n \tag{38}$$

The total contact area is given by

$$f(x) = 4b \cdot \left(1 - \frac{x^n}{a^n}\right)^n \tag{39}$$

Uneven ground

When a tyre is run over uneven ground there will be different types of contacts between the tyre and ground.

Figure 27.
Different types of tyre-ground contact

One way of calculating the contact area is to use the spring elements in the tyre model. Each spring element in contact with the ground has an area A associated with it.

The total area for one disc number 1–3 is given by:

$$A_m = AN \qquad m = 1,2,3 \tag{40}$$

where N is the number of elements in contact with the ground.

The total area for one disc number 4 and 5 is given by:

$$A_m = \frac{A}{2} N \qquad m = 4,5 \tag{41}$$

where N is the number of elements in contact with the ground.

The total contact area is given by:

$$A_{tot} = \sum_{m=1}^{5} A_m \tag{42}$$

The size of area A is determined from tyre area measurements.

Terrain model

The terrain model (Anon., 1994) is a general three-dimensional surface that is defined as a series of triangular patches as shown in figure 28.

Figure 28.
Terrain representation in ADAMS.

Figure 28 depicts a road surface formed by six nodes, numbered 1 through 6. The six nodes together form a triangular patch element denoted as A, B, C, and D. The unit outward normal for each triangular patch is shown for the sake of clarity. The road is specified by the co-ordinates of each node in a specified co-ordinate system. Subsequently the connectivity defining each triangular patch is specified. For each triangular patch, separate friction properties can also be specified.

In off-road applications there will be stones, rocks and stumps. These obstacles can be described by using triangular patches. There will be many small patches (see Fig. 29) when describing a stone, for example, which looks like a paraboloid of revolution.

Figure 29.
Description of a stone by using triangular patches.

When a tyre is run over an obstacle, like the stone in Fig. 29, the tyre will be in contact with more than two triangular patches at the same time. In ADAMS there is a restriction stipulating that the tyre cannot be in contact

with more than two patches at the same time. To avoid this restriction a new way to represent an obstacle in ADAMS is presented.

By using interpolation (Press, 1994) in two dimensions we can transform the triangular patches into a grid. In two dimensions we are given a matrix of functional values $y_a(j,k)$, where j varies from 1 to m, and k varies from 1 to n. We are also given an array x_{1a} of length m and an array x_{2a} of length n. The relation of these input quantities to an underlying function $y(x_1,x_2)$ is

$$y_a(j,k) = y(x_{1a}(j), x_{2a}(k)) \text{ s} \tag{43}$$

We want to estimate, by interpolation, the function y at some untabulated point (x_1,x_2).

An important concept is that of the grid square in which the point (x_1,x_2) falls; that is, the four tabulated points can surround the desired interior point. For convenience, we will number these points from 1 to 4, counterclockwise starting from the lower left, see Fig. 30.

Figure 30.
Labelling of points used in the two-dimensional interpolation routines.

Figure 31.
For each of the four points, you supply one function value, two first derivatives and one cross-derivative.

For each point you submit four values. In this case the function value is the height of the road in z-direction, the derivatives *z/x* and *z/y* and a friction value.

More precisely

$$x_{1a}(j) \le x_1 \le x_{1a}(j+1) \tag{44}$$
$$x_{2a}(j) \le x_2 \le x_{2a}(j+1) \tag{45}$$

defines j and k, then

$$y_1 \equiv y_a(j,k) \tag{46}$$
$$y_2 \equiv y_a(j+1,k) \tag{47}$$
$$y_3 \equiv y_a(j+1,k+1) \tag{48}$$
$$y_4 \equiv y_a(j,k+1) \tag{49}$$

The bilinear interpolation formulas are:

$$t \equiv (x_1 - x_{aj}(j)) \,/\, (x_{1a}(j+1) - x_{1a}(j)) \tag{50}$$
$$u \equiv (x_2 - x_{2j}(k)) \,/\, (x_{2a}(k+1) - x_{2a}(k)) \tag{51}$$

so that t and u each lie between 0 and 1, and

$$y(x_1,x_2) = (1-t)(1-u)y_1 + t(1-u)y_2 + tuy_3 + (1-t)uy_4 \tag{52}$$

As the interpolating point wanders from grid square to grid square, the interpolated function value changes continuously. However, the gradient of the interpolated functions changes discontinuously at the boundaries of each grid square.

A software programme has been developed to convert, by interpolation, the ADAMS road data format to grid square format. To avoid the problem with the gradient discontinuities at the boundaries a smoothing function has been developed and included in the software.

Each boundary point in a square grid is surrounded by 3, 5 or 8 points from the same square grid and from neighbouring square grids, Fig. 32.

Figure 32.
Each point is surrounded by 3, 5, or 8 points.

The smoothing function has been developed to avoid the problem with the gradient discontinuities at the boundaries. This function works as follows. If the boundary point (x_n, y_n) with a *z*-value is going to be smoothed out, the *z*-value for this point is multiplied by the value 1- *eps, eps* < 1, and the surrounding boundary point *z*-values are multiplied by 1 + *eps*.

Figure 33.
An obstacle expressed in ADAMS regular triangular format.

Figure 34.
Same obstacle as in Fig. 33 with the new interpolated format.

Figure 35.
Derivatives $\delta z/\delta x$ for the same obstacle as in Fig. 33.

Figure 36.
Derivatives $\delta z/\delta y$ for the same obstacle as in Fig. 33.

Machine model

The forest machine that has been modelled is a forwarder. The forwarder is manufactured by SISU Logging and is called Valmet 840. It is an articulated, 8-wheeled, all-wheel-drive machine with bogies in the rear and in the front, Fig. 37.

Figure 37.
The forwarder Valmet 840.

The forwarder has been built up in ADAMS, Fig. 38.

Figure 38.
The Valmet 840 modelled in ADAMS.

The forwarder consists of 32 rigid parts, 13 fixed joints, 1 translational joint, 12 revolute joints, 1 spherical joint and 1 universal joint. Each part has a mass and moment of inertia.

The revolute joints are (Fig. 39):

- joints connecting the tyres to the bogies.
- joints connecting the rear bogie arms to the rear bogie.
- joints connecting the front bogie arms to the front bogie.

Figure 39.
Revolute joints on the forwarder.

The spherical, translational and universal joints are for steering the articulation, see Fig 40.

Figure 40.
Spherical, translational and universal joints on the forwarder.

Fixed joints are used to connect rigid parts that do not move relative to each other. The fixed joints are (Fig. 41):

Figure 41.
Fixed joints on the forwarder.

Ground model

When comparing the results from the simulations with reality, fixed tracks with fixed obstacles have been used. The test site is located at P10, Strängnäs, Fig. 42. The test site consists of six different tracks.

Figure 42.
View of the test site at P10, Strängnäs.

Data on the test tracks have been collected with a geodemeter. A computer programme has been developed to convert data from the geodemeter into ADAMS triangular road data format. Fig. 43 shows an example of test track NR 5 in reality, and Fig. 44 shows the same test track in ADAMS.

Figure 43.
Photo of test track NR 5.

Figure 44.
Test track NR 5 in ADAMS with regular ADAMS triangular definition.

Figure 45
Test track NR 5 in ADAMS with the new interpolated definition.

Results

This chapter describes the results.

Dynamic tyre tests

Figure 46 shows an example of the result from the dynamic test rig.

Figure 46.
Result from the dynamic test rig.

Static tyre tests

Here are the results from the static tests with different loads and inflation pressures.

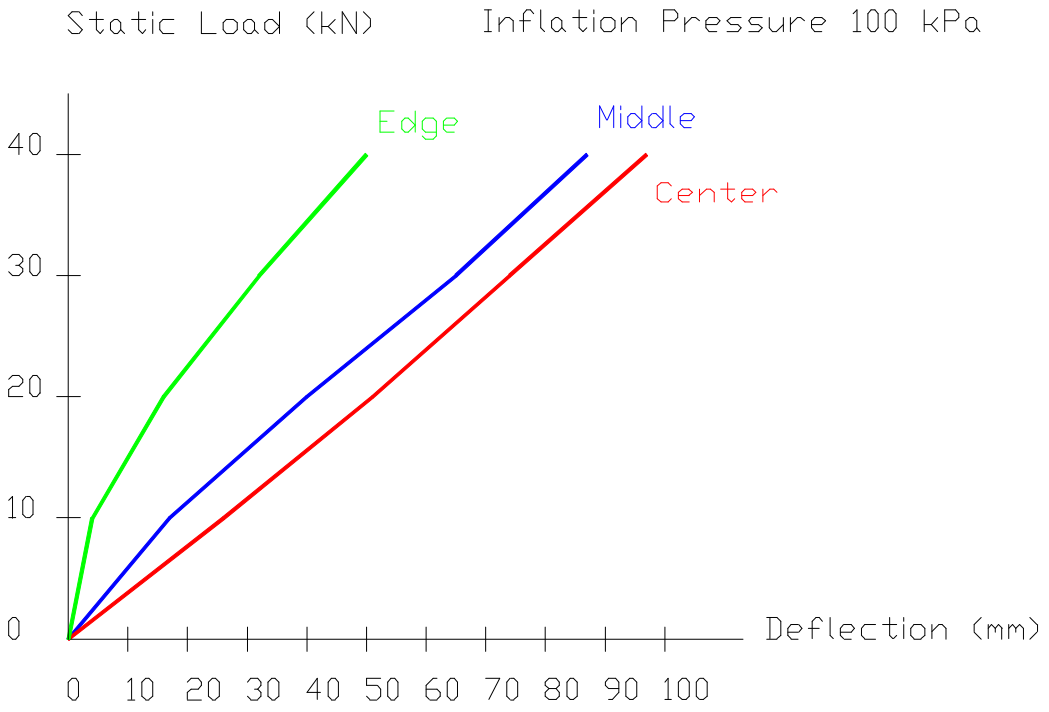

Figure 47.
Force - deflection, 100 kPa.

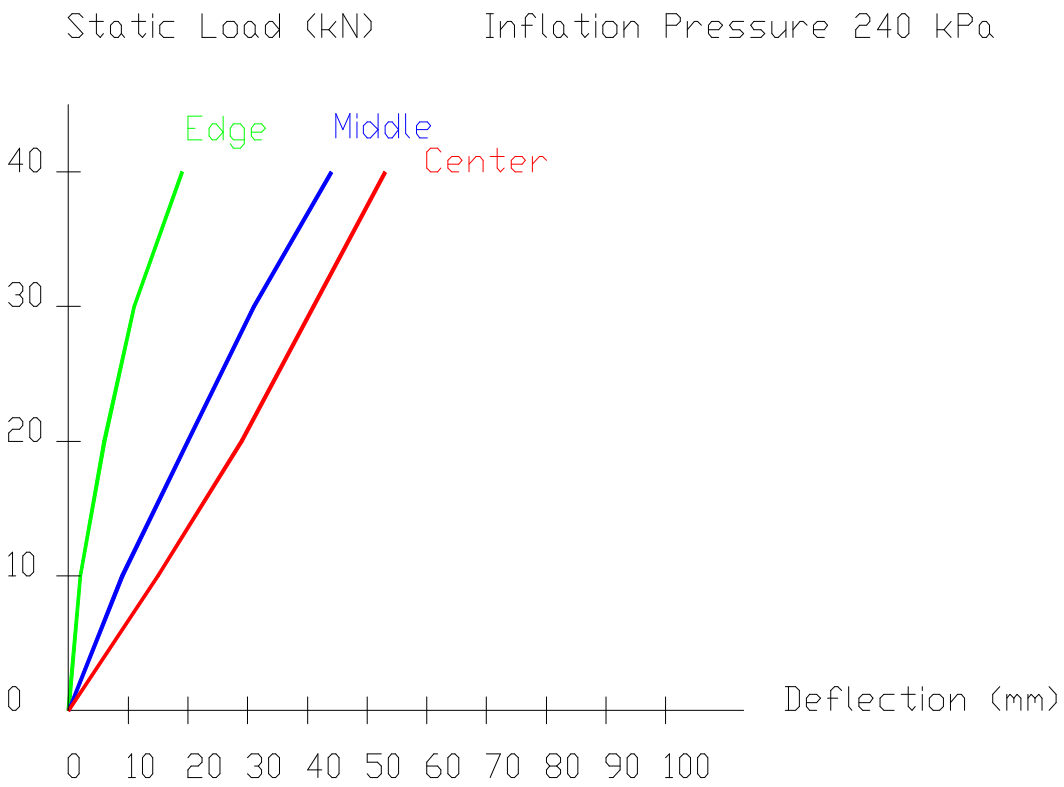

Figure 48.
Force - deflection, 240 kPa.

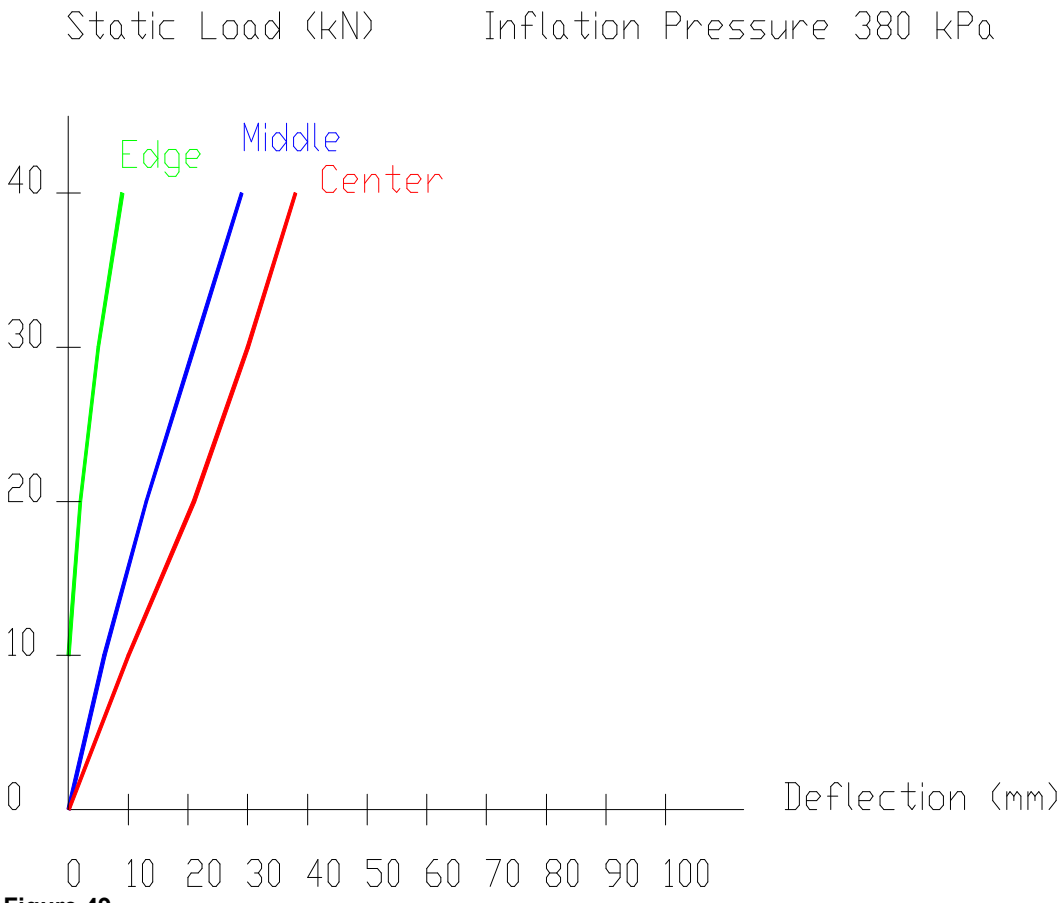

Figure 49.
Force - deflection, 380 kPa.

Area measurements

Super ellipse

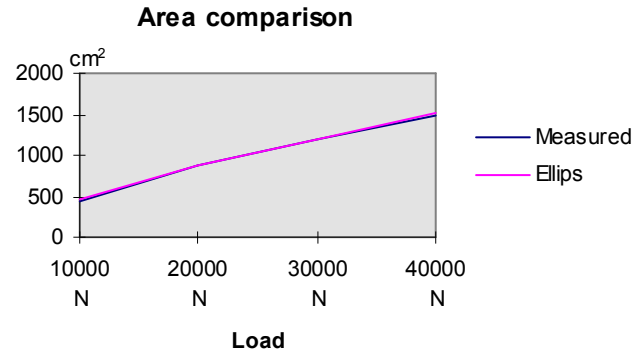

Figure 50.
Comparison of contact area between super-ellipse and planimeter.

Dynamic area

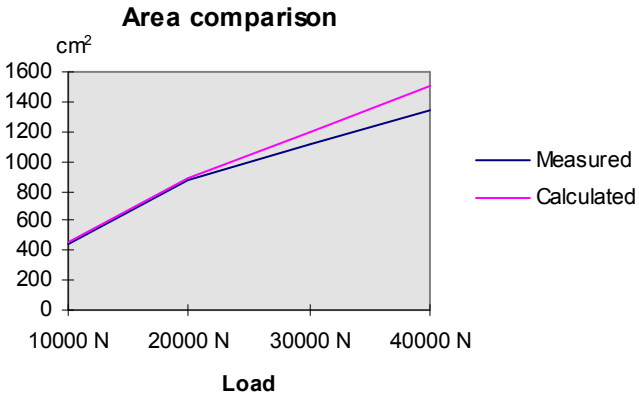

Figure 51.
Comparison of contact area between dynamic area and planimeter.

Practical tests

Track number 5

No payload

Figure 52.
Bogie angels on front bogies, 100 kPa

Figure 53.
Bogie angels on rear bogies, 100 kPa

With payload

Figure 54.
Bogie angels on front bogies, 100 kPa

Figure 55.
Bogie angels on rear bogies, 100 kPa

Conclusions

A new concept on describing the dynamic behaviour of a forwarder has been introduced. The simulation model consists of three major parts:

- the machine model
- the tyre model

A 3D tyre model for off-road application and a new ground model have been introduced. The tyre model is capable of running over uneven obstacle such as stones at low speed. The tyre model can predict tyre vertical, lateral and longitudinal forces. In its present form it may be suitable for some common forest machine simulation purposes, one its main attractions being its small amount of simply obtained experimental data which it demands. Based on comparisons with tyre test data it can be concluded that the tyre model duplicates the enveloping characteristics of forest tyre. However, verification has only been achieved for low speed tyre excursions. The significans of high rolling speed tyres in terms of the contribution of carcass dynamics to the net tyre loads is not known.

At this stage the tyre model is not fully completed. A full description and a more detailed discussion of the tyre model and demonstration of results will be presented in a thesis which is in preparation.

References

Anon. 1989. ADAMS Tire User manual. Version 5.2.1. Mechanical Dynamics Inc USA.

Anon. 1994. ADAMS Tire option manual. Version 8.0. Mechanical Dynamics Inc. USA.

Akima, H. 1970 A New method of interpolation and smooth curve fitting based on local procedures. Journal of the Association for computer machinery 17(4):589–602.

Badalamenti J. M., (1988) Radial-interradial spring tire models. Transaction of ASME, Vol.110, pp70–75.

Baladi, G. & Rohani, B. 1984. Development of soil-wheel interaction model. Proceedings of 8th Int. Conf. of ISTVS. pp 33 – 60.

Davis, D.C. 1974. A radial-spring terrain-envelopping tire model. Vehicle system dynamics 3:55-69

Fiala, E. 1964. Sietenkrafte am rollenden Luftreifen. VDI-Zeitschrift 96, 973

Friman, E. Et al. 1991. Design and test of controlled all hydrostatic transmission on a forwarder. Swedish University of Agricultural Sciences, Uppsatser och Resultat nr 201. Garpenberg.

Hallonborg, U. 1983. Bärighetsprov Hornborgasjön. Skogsarbeten. Resultat No. 4, 1983.

Hallonborg, U. 1996.

Ingram, W. F. 1973. A numerical model of the ride dynamics of a vehicle using a segmented tire concept. US Army Waterways Experiment station, TRM-73-5.

Karlsson, L. & Myhrman, D. 1990. Spårdjupsprov, engreppsskördare. SkogForsk. Resultat No. 22, 1990.

Karlsson, L. & Myhrman, D. 1990. Spårdjupsprov, skotare. SkogForsk. Resultat No. 23, 1990.

Kilner J. R. (1982) Tire model for aircraft simulation. Journal of Aircraft. Vol. 19. No 10, pp 851–857.

Löfgren B. 1992 Soil-tyre interface models. Bulletin No. 20. The Forest Research Institute of Sweden.

Löfgren, B. 1991. Lägre lufttryck ger mindre spårdjup. . SkogForsk. Resultat No. 23, 1991.

Olsen, H.-J. & Wästerlund. I. 1989. Terrain and vehicle research with referens to forestry at the Swedish University of Agricultural Sciences. Uppsatser och resultat nr 149. Garpenberg 1989.

Pacejka H. B. & Bakker, E.1993. The magic formula model.

Press, W. H. 1994. Numerical recipes in fortran. Cambridge University Press.